09/754,310

Patent Office
Canberra

I, CASSANDRA RICHARDS, ACTING TEAM LEADER EXAMINATION SUPPORT & SALES hereby certify that annexed is a true copy of the Provisional specification in connection with Application No. PQ 9157 for a patent by CANON KABUSHIKI KAISHA filed on 03 August 2000.

WITNESS my hand this
Twelfth day of January 2001

CASSANDRA RICHARDS
ACTING TEAM LEADER
EXAMINATION SUPPORT & SALES

CERTIFIED COPY OF PRIORITY DOCUMENT

S&F Ref: 504654

ORIGINAL

AUSTRALIA

Patents Act 1990

PROVISIONAL SPECIFICATION FOR THE INVENTION ENTITLED:

Self-Calibrating Method for Phase Estimation from Multiple Phase-Shifted Patterns

---

Name and Address of Applicant:

Canon Kabushiki Kaisha, incorporated in Japan, of 30-2, Shimomaruko 3-chome, Ohta-ku, Tokyo, 146, Japan

Name of Inventor:

Kieran Gerard Larkin

This invention is best described in the following statement:

SELF-CALIBRATING METHOD FOR PHASE ESTIMATION FROM MULTIPLE PHASE-SHIFTED PATTERNS

Technical Field of the Invention

The present invention relates to phase demodulation, and in particular to phase demodulation of a sequence of fringe patterns with arbitrary and unknown phase shifts between them. Such patterns typically occur in optical interferograms, but can also occur in interferograms produced by more general waves such as acoustic, synthetic aperture radar (SAR), ultrasound, and x-ray. More general image sequences, such as video, can in some cases also be modelled as fringe pattern sequences.

Background Art

Interferometry refers to experiments involving the interference of two light waves that have suffered refraction, diffraction or reflection in the interferometer. Such experiments typically involve the testing of lenses, mirrors and other optical components. The principle parameter of interest in interferometry is the phase difference between interfering beams.

Present methods of demodulating sequences of phase-related fringe-patterns generally rely on *a priori* knowledge of the phase-shifts between each of the individual patterns. When these relative phase-shifts are available, it is possible to estimate the spatial phase by using a generalised phase-shifting algorithm (PSA). In cases where the relative phase-shifts are not *a priori* known, the estimated spatial phase will be incorrect unless special error-reducing PSAs are used or methods to estimate the actual phase-shift between patterns are used.

Error-reducing PSAs are useful where the deviation of the actual phase-shift from the expected phase-shift is small (typically less than 0.1 radian) and deterministic. When the phase-shift deviation is larger and/or non-deterministic (ie essentially random), then other methods must be used.

Methods have been developed to estimate phase shifts between phase-related fringe patterns. Certain of the methods, based on statistical (least squares) estimation, requires at least 5 fringe patterns to work. Methods based on fitting the phase shifts to an ellipse also require at least 5 fringe patterns. Methods based on the statistical properties

of spatial phase histograms have been proposed, but are heavily dependent on certain restrictive, and often unrealistic criteria. More recently methods based upon the correlation between patterns have been proposed but are very sensitive to the number of full fringes in the frames. These correlation methods assume that the fringes are essentially linear in the frame, which means only trivial fringe patterns can be processed. Methods based on the maximum and minimum variation of individual pixels in different patterns typically require at least 15 frames to operate effectively.

In summary, current methods are unsatisfactory in many situations, especially for a small number of phase-related fringe-patterns, and many algorithms do not work in the case of three or four frames.

Disclosure of the Invention

It is an object of the present invention to substantially overcome, or at least ameliorate, one or more disadvantages of existing arrangements.

According to a first aspect of the invention, there is provided a method of estimating relative phase shifts between fringe pattern images in a sequence of phase-related fringe patterns, said method comprising the steps of:

a) removing offsets from each of said fringe pattern images to obtain pure AMFM patterns;

b) determining contingent analytic images corresponding to each of said AMFM patterns;

c) determining phase differences from dependent pairs of said contingent analytic images; and

d) estimating phase shifts between pairs of said contingent analytic images, wherein said phase shifts between pairs of said contingent analytic images are said relative phase shifts between fringe pattern images.

According to a second aspect of the invention, there is provided a method of estimating a spatial phase of fringe pattern images in a sequence of fringe patterns, said method comprising the steps of:

a) removing offsets from each of said fringe pattern images to obtain pure AMFM patterns;

b) determining contingent analytic images corresponding to each of said AMFM patterns;

c) determining phase differences from dependent pairs of said contingent analytic images;

d) estimating phase shifts between pairs of said contingent analytic images; and

e) estimating a spatial phase of said fringe pattern images.

According to another aspect of the invention, there is provided an apparatus for implementing any one of the aforementioned methods.

According to another aspect of the invention there is provided a computer program product including a computer readable medium having recorded thereon a computer program for implementing any one of the methods described above.

Brief Description of the Drawings

A preferred embodiment of the present invention will now be described with reference to the drawings, in which:

Fig. 1 shows the local structure of a typical fringe pattern;

Fig. 2 shows the Fourier domain coordinates;

Figs. 3A and 3B show the phase shift parameters δ_n for the case where N=5 on a polar plane;

Fig. 4 shows a flowchart of an automatic calibration method in accordance with a preferred embodiment;

Fig. 5 shows an example of a fringe pattern;

Fig. 6A and 6B show the magnitude and phase components respectively of an analytic image of the example fringe pattern shown in Fig. 5;

Fig. 7A shows a phase difference between dependent analytic images;

Fig. 7B shows a histogram of a spread in values of the phase difference shown in Fig 7A;

Fig. 8A shows a modulus of the phase difference between dependent analytic images shown in Fig. 7A;

Fig. 8B shows a histogram of a spread in values of the modulus of the phase difference shown in Fig. 8B;

Fig. 9 shows a polarity function calculated from the phase difference shown in Fig. 7A and the modulus of the phase difference shown in Fig. 8A;

Figs. 10A and 10B show estimations of an amplitude modulation and a phase of the fringe pattern shown in Fig. 5;

Fig. 11 shows an estimate of an offset of the fringe pattern shown in Fig. 5;

Fig. 12 shows a simple weight function calculated from the estimated errors in the analytic image shown in Figs. 6A and 6B; and

Fig. 13 shows a schematic block diagram of a general purpose computer upon which the preferred embodiment of the present invention can be practiced.

Detailed Description including Best Mode

Interferometry is the use of interference phenomena for measurement purposes. This allows for the measurement of very small angles or small displacements of objects relative to one another. An interferometer is a device to make such measurements, which typically uses a beam of light, coming from a single source, such as a star, a laser or a lamp, and two or more flat mirrors to split off different light beams. These beams are then combined so as to 'interfere' with each other. The beams interfere with each other by constructively adding together and cancelling each other out, thereby forming alternating bands of light and dark, called fringe patterns.

What makes the interferometer such a precise measuring instrument is that these fringes are only one light-wavelength apart, which for visible light corresponds to about 590 nm. With the fringe patterns having a cyclic nature with phases that shifted, the important measurement parameter is the relative phase-shifts between these phase-related fringe patterns.

Consider an intensity $f_n(x,y)$ of the n^{th} fringe pattern in a sequence of phase-related fringe patterns with the following mathematical form:

$$f_n(x,y) = a(x,y) + b(x,y)\cos\left[\psi(x,y) + \delta_n\right] \tag{1}$$

wherein $a(x,y)$ is a background or offset, $b(x,y)$ is the amplitude modulation, and $\psi(x,y)$ is the phase. Each fringe pattern has a phase shift parameter δ_n. An example of such a fringe pattern is shown in Fig. 5.

A improved method of estimating relative phase-shifts between phase-related fringe patterns f_n is proposed. The method is based on an isotropic quadrature transform. The isotropic quadrature transform is used to estimate the spatial phase $[\psi(x,y)+\delta_n]$ in one fringe pattern f_n, followed by comparing the spatial phase $[\psi(x,y)+\delta_n]$ between fringe patterns f_n to estimate the relative phase-shift(s). With 3 or more frames, the method is independent of background variations $a(x,y)$.

The exact value of phase $\psi(x,y)$ can be calculated from three or more fringe patterns f_n if the values of the phase shift parameter δ_n is known for each fringe pattern f_n. For more than three fringe patterns $f_n(x,y)$, the phase $\psi(x,y)$ is over-determined and is usually estimated in a maximum likelihood process. Other estimation processes may be more appropriate in cases where additional systematic error or distortion effects apply to Equation (1).

Consider a least squares estimate for the phase $\psi(x,y)$ from N fringe patterns:

$$\begin{pmatrix} \sum 1 & \sum c_n & \sum s_n \\ \sum c_n & \sum c_n^2 & \sum c_n s_n \\ \sum s_n & \sum c_n s_n & \sum s_n^2 \end{pmatrix} \begin{pmatrix} a \\ +b\cos\psi \\ -b\sin\psi \end{pmatrix} = \begin{pmatrix} \sum f_n \\ \sum c_n f_n \\ \sum s_n f_n \end{pmatrix} \tag{2}$$

where $c_n = \cos\delta_n$, and $s_n = \sin\delta_n$, and the summations are over N fringe patterns ie. $\sum = \sum_{n=1}^{N}$. Least squares Equation (2) can be inverted, providing c_n and s_n are such that a singular matrix does not occur, as follows:

$$\begin{pmatrix} a \\ +b\cos\psi \\ -b\sin\psi \end{pmatrix} = \begin{pmatrix} \sum 1 & \sum c_n & \sum s_n \\ \sum c_n & \sum c_n^2 & \sum c_n s_n \\ \sum s_n & \sum c_n s_n & \sum s_n^2 \end{pmatrix}^{-1} \begin{pmatrix} \sum f_n \\ \sum c_n f_n \\ \sum s_n f_n \end{pmatrix} \tag{3}$$

Equation (3) allows for the offset $a(x,y)$, the amplitude modulation $b(x,y)$, and the phase $\psi(x,y)$ to be calculated. However, before Equation (3) can be used, all the phase shift parameters δ_n must be known.

The phase shift parameter δ_n of each fringe pattern is estimated by using a 2-D quadrature technique based on a spiral phase Fourier operator. Estimation of phase

$\psi(x,y)$ in the above manner has many advantages related to the extraordinary demodulation properties of the spiral phase Fourier operator.

A first step in determining the phase shift parameters δ_n is to remove the background (offset) $a(x,y)$ from each of the fringe patterns $f_n(x,y)$. In the preferred embodiment, this is done by forming inter-frame differences between pairs of fringe patterns $f_n(x,y)$ as follows:

$$g_{nm} = f_n - f_m = -g_{mn} = b\{\cos[\psi + \delta_n] - \cos[\psi + \delta_m]\} \tag{4}$$

The inter-frame difference function g_{nm} is a pure AMFM (amplitude modulation and frequency modulation) function without offset and therefore can be demodulated if the inter-frame difference function g_{nm}, which is also a fringe pattern, is locally simple. For the fringe pattern g_{nm} to be locally simple, it has to have a unique orientation $\beta(x,y)$ and spacing $\lambda(x,y)$ at each location (x,y), except, perhaps, at a finite number of locations where the orientation $\beta(x,y)$ and/or spacing $\lambda(x,y)$ may be uncertain. Advantageously, local simplicity is a property which distinguishes fringe patterns from other, more general, patterns. Fig. 1 shows the local structure of a typical fringe pattern indicating the orientation $\beta(x,y)$ and spacing $\lambda(x,y)$ for the small region.

A spiral phase Fourier operator V{}, hereinafter referred to as a vortex operator, is defined as follows:

$$\begin{aligned}
&\mathrm{V}\{f(x,y)\} = \mathrm{F}^{-1}\{\exp[i\phi]\mathrm{F}\{f(x,y)\}\} \\
&\mathrm{F}\{f(x,y)\} = F(u,v) = \int_{-\infty}^{+\infty}\int_{-\infty}^{+\infty} f(x,y)\exp[-2\pi i(ux+vy)]\,dxdy \\
&\mathrm{F}^{-1}\{F(u,v)\} = f(x,y) = \int_{-\infty}^{+\infty}\int_{-\infty}^{+\infty} F(u,v)\exp[+2\pi i(ux+vy)]\,dudv \\
&\left.\begin{aligned} u &= q\cos\phi \\ v &= q\sin\phi \end{aligned}\right\}
\end{aligned} \tag{5}$$

The Fourier operator F{ } transforms a general function *f(x,y)* from the spatial domain (x,y) to the spatial frequency domain (u,v). The Inverse Fourier operator F^{-1}{ } transforms a spatial frequency domain signal back to the spatial domain (x,y). In

practice, for discretely sampled images, the Fourier and the Inverse Fourier transforms are efficiently performed by a Fast Fourier transform algorithm and an Inverse Fast Fourier transform algorithm.

The spiral phase $\exp[i\phi]$ is wholly a function of the angular component of the spatial frequency polar coordinates (q,ϕ) shown in Fig. 2. The vortex operator V{} is applied to the inter-frame difference functions g_{nm} to obtain:

$$\mathrm{V}\{g_{mn}\} \cong i\exp[i\beta]b\left[\sin(\psi+\delta_n)-\sin(\psi+\delta_m)\right] \tag{6}$$

From Equation (6) it can be seen that the vortex operator V{} is an isotropic quadrature operator in that it converts cosine fringes at any orientation $\beta(x,y)$ into sine fringes at the same orientation $\beta(x,y)$. The approximation in Equation (6) is valid except in regions where the amplitude modulation $b(x,y)$, spacing $\lambda(x,y)$ or orientation $\beta(x,y)$ vary too rapidly. Areas where the radius of curvature of the fringe pattern g_{nm} is smaller than the fringe spacing $\lambda(x,y)$ also give a lower accuracy approximation. However, for most typical fringe patterns g_{nm}, the approximation is good and any errors are isotropically distributed. In contrast, conventional methods, such as the half-plane Hilbert transform, cause highly directional errors, and are not suitable for high precision demodulation of general fringe patterns.

Next, the local orientation $\beta(x,y)$ is compensating for. To do so, the orientation $\beta(x,y)$ must be estimated. There are a number of ways to do this. One method relies on the gradient of the fringe pattern g_{nm}. The ratio of the x and y components gives the tangent angle $\beta(x,y)$ from the local Taylor's series expansion of the phase $\psi(x,y)$ about the point (x_0,y_0):

$$\begin{aligned}
&\psi(x,y)=\psi_{00}+2\pi u_0(x-x_0)+2\pi v_0(y-y_0)+O(r^2)\\
&\left.\frac{\partial\psi(x,y)}{\partial x}\right|_{\substack{x=x_0\\y=y_0}} \cong 2\pi u_0\\
&\left.\frac{\partial\psi(x,y)}{\partial y}\right|_{\substack{x=x_0\\y=y_0}} \cong 2\pi v_0
\end{aligned} \tag{7}$$

The gradient components are:

$$\frac{\partial g_{nm}}{\partial x} \cong b\left(-\sin\left(\psi+\delta_n\right)+\sin\left(\psi+\delta_m\right)\right)\frac{\partial \psi}{\partial x}$$
$$\frac{\partial g_{nm}}{\partial y} \cong b\left(-\sin\left(\psi+\delta_n\right)+\sin\left(\psi+\delta_m\right)\right)\frac{\partial \psi}{\partial y} \tag{8}$$

The ratio of the gradient components gives the tangent angle:

$$\frac{\partial g_{nm}}{\partial y}\Big/\frac{\partial g_{nm}}{\partial x} \cong \frac{v_0}{u_0} = \tan\beta_{nm} \tag{9}$$

Again the approximation of Equation (9) is valid in regions with smoothly varying parameters as defined for the vortex operator $\mathrm{V}\{\}$. Other methods of orientation estimation may be used. For example, methods based on the multi-dimensional energy operator or the vortex operator itself may be used. Generic orientation estimation is assumed at this point, and the orientation β for any fringe pattern f_n or inter-frame difference function g_{nm} may be calculated. Alternatively the orientation β may be estimated from combinations of the previous methods in a statistically advantage manner. It will be assumed hereinafter that there is just one orientation estimate, which shall be called orientation estimate β_e. The orientation estimate β_e typically contains an ambiguity in the sign:

$$\exp[i\beta] = \cos\beta + i\sin\beta = \pm\frac{u_0+iv_0}{\sqrt{u_0^2+v_0^2}} \tag{10}$$

Different orientation estimates β_e typically have the sign ambiguities in different places. It is worth noting that the overall sign ambiguity arises from the general difficulty in distinguishing a fringe at orientation β from a fringe at orientation $\beta+\pi$.

Equation (4) is rewritten as:

$$g_{nm} = 2b\sin\left[\psi+\left(\delta_m+\delta_n\right)/2\right]\sin\left[\left(\delta_m-\delta_n\right)/2\right] \tag{11}$$

and Equation (6) as:

$$\exp\left[-i\beta_e\right]\mathrm{V}\left\{g_{nm}\right\} \cong 2ib\exp\left[i\left(\beta-\beta_e\right)\right]\cos\left[\psi+\left(\delta_m+\delta_n\right)/2\right]\sin\left[\left(\delta_m-\delta_n\right)/2\right] \tag{12}$$

The complex exponential in Equation (12) has possible values {-1;1}, depending on the orientation estimate β_e, and shall be called a polarity factor $h(x,y)$:

$$h(x,y) = \exp\left[i(\beta - \beta_e)\right] \tag{13}$$

A contingent analytic image $\breve{g}_{nm}$ is defined as:

$$\breve{g}_{nm} = i(g_{nm} - \exp[-i\beta_e]\mathrm{V}\{g_{nm}\}) \tag{14}$$

By substituting Equations (11), (12) and (13) into Equation (14), the contingent analytic image $\breve{g}_{nm}$ is rewritten as:

$$\breve{g}_{nm} \cong 2b\sin[(\delta_m - \delta_n)/2](h\cos[\psi + (\delta_m + \delta_n)/2] + i\sin[\psi + (\delta_m + \delta_n)/2]) \tag{15}$$

This definition of an analytic image is contingent upon the orientation function β_e used in the definition shown in Equation (14). It is noted that the contingent analytic image $\breve{g}_{nm}$ can be achieved by placing the inter-frame difference function g_{nm} in the imaginary part of a complex image, and placing the imaginary output of the vortex operator $\mathrm{V}\{\}$ in the real part.

A phase α_{nm} of the contingent analytic image $\breve{g}_{nm}$ is calculated as follows:

$$\alpha_{nm} = Arg\left\{ig_{nm} - i\exp[-i\beta_e]\mathrm{V}\{g_{nm}\}\right\} \cong h\left[\psi + (\delta_m + \delta_n)/2\right] \tag{16}$$

The calculation of phase α_{nm} is possible as long as $\sin\left[(\delta_m - \delta_n)/2\right] \neq 0$, which only occurs if $\delta_m - \delta_n \neq 2\pi j$ where j is an integer. Clearly the failure to calculate phase α_{nm} in such a case is due to the phase shifts δ_m and δ_m being essentially equal and the inter-frame difference function g_{nm} being identically zero.

The phase difference between dependent pairs of contingent analytic images, such as $\breve{g}_{nm}$ and $\breve{g}_{mk}$, is calculated as follows:

$$\alpha_{nm} - \alpha_{mk} = h\left[\psi + (\delta_m + \delta_n)/2\right] - h\left[\psi + (\delta_k + \delta_m)/2\right] = h\left[(\delta_n - \delta_k)/2\right] \tag{17}$$

This allows a difference in phase between any two fringe patterns f_n and f_k to be found, namely (δ_n-δ_k), with a sign ambiguity as a result of the polarity factor h. It is noted that all phase calculations, including phase differences, are calculated modulo 2π. Various methods may be used to extract both the polarity factor h and the phase

differences (δ_n-δ_k). In a simplest embodiment, from Equation (17), the absolute values of the phase difference between two fringe patterns f_n and f_k are averaged over the full fringe pattern area S:

$$|\delta_n - \delta_k|_{mean} = 2\frac{\iint_S |\alpha_{nm} - \alpha_{mk}| dxdy}{\iint_S dxdy} \tag{18}$$

A preferred embodiment uses a weighted integral with weighting $w(x,y)$ over the fringe pattern area S. The weighting $w(x,y)$ used should be a measure of the estimated accuracy of the local estimate of the phase α_{nm}. This is related to the AMFM characteristics of the fringe patterns $f_n(x,y)$ in the sequence of phase-related fringe patterns. Thus, the absolute values of the phase difference (δ_n-δ_k) between two fringe patterns f_n and f_k, weighted averaged over the full fringe pattern area S is:

$$|\delta_n - \delta_k|_{\substack{weighted \\ mean}} = 2\frac{\iint_S |\alpha_{nm} - \alpha_{mk}| w^2(x,y) dxdy}{\iint_S w^2(x,y) dxdy} \tag{19}$$

This allows for a very low (or zero) weighting $w(x,y)$ to be used where the phase α_{nm} varies quickly, as is the case for discontinuities, or areas where the modulation $b(x,y)$ is low. Equation (17) can be rewritten as:

$$\frac{\alpha_{nm} - \alpha_{mk}}{|\alpha_{nm} - \alpha_{mk}|} = h(x,y)\frac{\delta_n - \delta_k}{|\delta_n - \delta_k|} \tag{20}$$

By arbitrarily taking the phase difference (δ_n-δ_k) for these particular values of n and k as positive, from Equation (20) follows an estimated polarity factor h_e as:

$$h_e(x,y) = \frac{\alpha_{nm} - \alpha_{mk}}{|\alpha_{nm} - \alpha_{mk}|} \tag{21}$$

This estimated polarity factor function h_e can be used in all further computations, because a global sign convention has effectively been set for the phase difference (δ_n-δ_k) in the fringe pattern sequence.

Next, the phase difference $\delta_n - \delta_k$ may be calculated for all possible pairs. The minimum requirement is to calculate the phase difference $\delta_n - \delta_k$ for all sequential pairs, which amounts to N values for N fringe patterns f_n. By also calculating the phase

difference $\delta_n - \delta_k$ for non-sequential pairs, additional statistical robustness in the estimates is achieved. The number of combinations of two-phase differences $\delta_n - \delta_k$ from N phases are:

$$\frac{N!}{2(N-2)!} \tag{22}$$

In the particularly interesting case where N=3, the number of combination is also 3, which equals the number of sequential differences too. Figs. 3A and 3B show the phase shift parameters δ_n for the case where N=5 on a polar plane. The points 1-5 are thus on a unity circle at points corresponding.to $\exp(i\delta_n)$. The connecting line between points n and m corresponds to $[\exp(i\delta_m)-\exp(i\delta_n)]$. The length of each connecting line is proportional to $\sin\left[(\delta_m - \delta_n)/2\right]$, which also appeared in the inter-frame difference function g_{nm} of Equation (11). The length of each connecting line is a direct indication of the reliability of the estimate of the phase difference $\delta_n - \delta_k$, as the length is the factor appearing in the magnitude of the inter-frame difference function g_{nm}. Fig. 3A shows the connecting lines for all sequential pairs, whereas Fig. 3B shows all possible connecting lines, and thus inter-frame differences $\delta_n - \delta_k$, which adds another 5 phase differences $\delta_n - \delta_k$. With the phase differences γ_{mn} defined as $\gamma_{mn} = \delta_m - \delta_n$, an estimation $\bar{\gamma}_{mn}$ of each of the phase differences γ_{mn} may be calculated using a weighted mean, and compensated by the estimated polarity h_e as follows:

$$\bar{\gamma}_{nk} = \left\{ 2 \frac{\iint_S h_e (\alpha_{nm} - \alpha_{mk}) w^2 dxdy}{\iint_S w^2 dxdy} \right\}_{\text{mod}2\pi} \tag{24}$$

In situations where the fringe patterns f_n contain noise and/or other distortions, the best phase differences estimates $\bar{\gamma}_{mn}$ may come from a two dimensional fit of all the points corresponding to $\exp(i\delta_n)$, as shown in Figs. 3A and 3B, to a unit radius circle.

Without loss of generality, one of the phase shift parameters δ_n may be set to zero. For convenience the first phase shift parameter $\delta_1 = 0$ is set. This is consistent with the idea that the absolute value of the phase $\psi(x,y)$ is undefined and only phase

differences $\gamma_{mn} = \delta_m - \delta_n$ are really meaningful. The remaining (relative) phase shift parameters $\bar{\delta}_n$ are calculated as follows:

$$\begin{aligned} \bar{\delta}_1 &= 0 \\ \bar{\delta}_2 &= \bar{\delta}_1 + \bar{\gamma}_{21} \\ \bar{\delta}_3 &= \bar{\delta}_2 + \bar{\gamma}_{32} \\ \bar{\delta}_4 &= \bar{\delta}_3 + \bar{\gamma}_{43} \\ \bar{\delta}_5 &= \bar{\delta}_4 + \bar{\gamma}_{54} \end{aligned} \tag{25}$$

These values of the phase shift parameters δ_n are substituted back into the general PSA defined by Equation (3). This allows for all the fringe pattern parameters, namely the offset $a(x,y)$, the amplitude modulation $b(x,y)$, and a phase $\psi'(x,y)$ to be calculated. It is noted that the calculated phase $\psi'(x,y)$ then includes a common phase shift, namely the phase shift δ_1.

However, there may be some residual calibration error due to the original vortex operator failing in certain areas. These errors are rectified by re-evaluating the weight function $w(x,y)$ based on the present estimates of the offset $a(x,y)$, the amplitude modulation $b(x,y)$, and phase $\psi'(x,y)$, as well as their partial derivatives. This allows for the assessment of how well the original fringe patterns, in the form of the inter-frame difference functions g_{nm}, fulfilled the smoothness requirements of the vortex operator V{}. Areas where the phase α_{nm} varies too quickly, or areas where the modulation $b(x,y)$ is too low, the weighting function $w(x,y)$ is reduced or set to zero. Once a new weight function $w(x,y)$ is formed, the phase calibration process, from Equation (19) onwards, is repeated, resulting in better estimates for the phase shift parameters $\bar{\delta}_n$.

The accuracy of the estimates for the phase shift parameters $\bar{\delta}_n$ may be expressed as the variance of phase difference, as follows:

$$\sigma^2_{\delta_n - \delta_k} = 4 \frac{\iint_S \left(|\alpha_{nm} - \alpha_{mk}| - \bar{\alpha}_{nk} \right)^2 w^2(x,y)\, dxdy}{\iint_S w^2(x,y)\, dxdy} \tag{26}$$

wherein

$$\bar{\alpha}_{nk} = \frac{\iint_S |\alpha_{nm} - \alpha_{mk}| w^2(x,y)\,dxdy}{\iint_S w^2(x,y)\,dxdy} \tag{27}$$

Care is needed in evaluating Equations (26) and (27), as the phase $\psi'(x,y)$ is periodic and false discontinuities can disrupt the calculations if $\bar{\alpha}_{nk}$ near $-\pi$ or π.

Other methods for estimating these parameters $\bar{\alpha}_{nk}$ that specifically incorporate the cyclic nature may be used instead of Equation (27), for example:

$$\bar{\alpha}_{nk} = \arg\left\{\iint_S \exp\left[i|\alpha_{nm} - \alpha_{mk}|\right] w^2(x,y)\,dxdy\right\} \tag{28}$$

Fig. 4 shows a preferred embodiment of a automatic phase-shift calibration method 100. A first step 110 receives a sequence of fringe patterns f_n. Each of the fringe patterns f_n is real valued. An example of one of the fringe patterns f_n from the sequence is shown in Fig. 5. Step 120 removes the fringe pattern offset $a(x,y)$ from each of the fringe patterns f_n. This is done by forming inter-frame differences g_{nm} as defined in Equation (4). The inter-frame differences g_{nm} are also real valued.

Step 130 forms analytic images $\breve{g}_{nm}$ corresponding to the inter-frame differences g_{nm} as defined in Equation (15). This is preferably achieved by placing the inter-frame difference function g_{nm} in the imaginary part of a complex image, and placing the imaginary output of the vortex operator $V\{g_{nm}\}$ in the real part. Fig. 6A and 6B show the magnitude and phase components respectively of an analytic image $\breve{g}_{nm}$ of the example fringe pattern f_n shown in Fig. 5. To enable the values of the phase components of the analytic image $\breve{g}_{nm}$ to be displayed, the values have been adapted to a range [0;255] with 0 representing $-\pi$ and 255 representing $\frac{127}{128}\pi$.

Step 140 extracts the phase difference $\alpha_{nm} - \alpha_{mk}$ (modulo 2π) from two dependent analytic images $\breve{g}_{nm}$ and $\breve{g}_{mk}$. Fig. 7A shows a phase difference $\alpha_{nm} - \alpha_{mk}$ between dependent analytic images $\breve{g}_{nm}$ and $\breve{g}_{mk}$ of the example fringe pattern f_n. Again, the values of the phase difference $\alpha_{nm} - \alpha_{mk}$ have been adapted to a range [0;255] with 0

representing $-\pi$ and 255 representing $\frac{127}{128}\pi$, allowing the values to be displayed. The dark areas 710 and 711 have values close to zero on the representation, which corresponds to values for close to $-\pi$ in the phase difference $\alpha_{nm}-\alpha_{mk}$, whereas the light areas 720 and 721 have values close to 255 in the representation, which corresponds to values close to π in the phase difference $\alpha_{nm}-\alpha_{mk}$. Accordingly, a value of 128 in the representation corresponds to a value of 0 in the phase difference $\alpha_{nm}-\alpha_{mk}$. The spread of values in the representation is shown in the histogram of Fig. 7B. The peaks 730 and 731 in the histogram corresponds to phase difference $\alpha_{nm}-\alpha_{mk}$ values.

Step 150 determines a modulus of the phase difference $|\alpha_{nm}-\alpha_{mk}|$. Fig. 8A shows the modulus $|\alpha_{nm}-\alpha_{mk}|$ of the phase difference $\alpha_{nm}-\alpha_{mk}$ represented in Fig. 7A. Again the values have been adapted to a range [0;255] with 0 representing $-\pi$ and 255 representing $\frac{127}{128}\pi$. As can be seen from Fig. 8A, all the values have a small variation. This is confirmed in the histogram shown in Fig. 8B, wherein the spread of values in the representation is shown. A single peak 810 in the histogram corresponds to modulus of phase difference $|\alpha_{nm}-\alpha_{mk}|$ values. It is noted that the values have only a small spread around the peak value.

Step 160 calculates the estimated polarity factor $h_e(x,y)$, using Equation (21). The result is shown in Fig. 9 wherein all regions have values –1 or 1, with the dark areas corresponding to values of –1 and the light areas corresponding to values of 1. The phase differences $\bar{\gamma}_{mn}$ are calculated using Equation (24) and the relative phase-shift parameters $\bar{\delta}_n=\bar{\delta}_{n-1}+\bar{\gamma}_{n(n-1)}$ are estimated in a consistent manner in step 170.

The relative phase-shift parameters $\bar{\delta}_n$ are then substituted into the general PSA defined by Equation (3) and the fringe pattern offset $a(x,y)$, the modulation $b(x,y)$, and phase $\psi'(x,y)$ are estimated in step 180. The resultant modulation $b(x,y)$, phase $\psi'(x,y)$ and offset $a(x,y)$ of the fringe pattern $f_n(x,y)$ of the example are shown in Figs. 10A, 10B and 11 respectively. It is noted that Figs. 10A and 11 appear almost uniformly white, which corresponds to almost no variation in the values of the modulation $b(x,y)$ and offset $a(x,y)$ with respect to coordinates (x,y) for the example shown.

Step 190 estimates the likely errors in the earlier contingent analytic images $\tilde{g}_{nm}$ and $\tilde{g}_{mk}$ by means of a direct comparison of the analytic image $\tilde{g}_{nm}$ and the PSA image. Step 192 determines whether these errors are higher than a preset threshold. If the errors are smaller than the threshold, the method 100 ends in step 196. If these errors are higher than the threshold, the errors are incorporated into the weighting $w(x,y)$ in step 194 and the method 100 returns to step 170 in an iterative manner, where the new weighting $w(x,y)$ is applied to the estimation of the mean phase-difference $\bar{\gamma}_{mn}$, until the errors are sufficiently low. In a simplest embodiment, the weighting $w(x,y)$ is set to 1 for co-ordinates *(x,y)* where the comparison is good and 0 where the comparison is poor.

Fig. 12 shows an example where the comparison of step 190 yields a weighting $w(x,y)$ which is 1.0 where the comparison is good and 0.0 where the comparison is poor.

It is generally noted that in equations with integrals over all values of x and y, such as Equations 5, 18, 19, 24 and 26, the integrals may be replaced by discrete summations for discretely sampled images.

A general-purpose computer system 100, upon which the preferred embodiment of the invention may be practised, is shown in Fig. 13. The method 100 can be implemented as software, such as an application program executing within the computer system 200. In particular, the steps of the method are effected by instructions in the software that are carried out by the computer system 200. The software may be stored in a computer readable medium, including the storage devices described below, for example. The software is loaded into the computer system 200 from the computer readable medium, and then executed by the computer system 200. A computer readable medium having such software or computer program recorded on it is a computer program product. The use of the computer program product in the computer preferably effects an advantageous apparatus for estimating the phase of a sequence of fringe patterns, in accordance with the embodiment of the invention.

The computer system 200 comprises a computer module 201, input devices such as a keyboard 202 and mouse 203, and output devices including a printer 215 and a display device 214. The computer module 201 typically includes at least one processor unit 205, a memory unit 206, for example formed from semiconductor random access memory (RAM) and read only memory (ROM), input/output (I/O) interfaces including a

video interface 207, an I/O interface for the printer device 215 and an I/O interface 213 for the keyboard 202 and mouse 203. A storage device 209 is provided and typically includes a hard disk drive 210 and a floppy disk drive 211. A CD-ROM drive (not illustrated) may be provided as a non-volatile source of data. The components 205 to 213 of the computer module 201, typically communicate via an interconnected bus 204 and in a manner which results in a conventional mode of operation of the computer system 200 known to those in the relevant art.

Typically, the application program of the preferred embodiment is resident on the hard disk drive 210, and read and controlled in its execution by the processor 205. Intermediate storage of the program may be accomplished using the semiconductor memory 206, possibly in concert with the hard disk drive 210. In some instances, the application program may be supplied to the user encoded on a CD-ROM or floppy disk and read via a CD-ROM drive (not illustrated) or floppy disk drive 211, or alternatively may be read by the user from the network (not illustrated) via the modem device (not illustrated). Still further, the software can also be loaded into the computer system 200 from other computer readable medium including magnetic tape, a ROM or integrated circuit, a magneto-optical disk, a radio or infra-red transmission channel between the computer module 101 and another device, a computer readable card such as a PCMCIA card, and the Internet and Intranets including e-mail transmissions and information recorded on websites and the like. The foregoing is merely exemplary of relevant computer readable mediums. Other computer readable mediums may be practiced without departing from the scope and spirit of the invention.

The method 100 of estimating the phase of a sequence of fringe patterns may alternatively be implemented in dedicated hardware such as one or more integrated circuits performing the functions or sub functions of estimating the phase of a sequence of fringe patterns. Such dedicated hardware may include graphic processors, digital signal processors, or one or more microprocessors and associated memories.

Industrial Applicability

The embodiment of the invention are applicable to interferometric testing of optical components and optical systems. The embodiment may also be used in non-destructive testing to study the deformation of objects under stress, and the study of

vibrating objects to identify vibration modes. Often, optical techniques are also used to visualise fluid flows, and variations in density are displayed in the form of fringe patterns.

The foregoing describes only one embodiment of the present invention, and modifications and/or changes can be made thereto without departing from the scope and spirit of the invention, the embodiment being illustrative and not restrictive.

In the context of this specification, the word "comprising" means "including principally but not necessarily solely" or "having" or "including" and not "consisting only of". Variations of the word comprising, such as "comprise" and "comprises" have corresponding meanings.

~~CLAIMS~~

The claims defining the invention are as follows:

1. A method of estimating relative phase shifts between fringe pattern images in a sequence of phase-related fringe patterns, said method comprising the steps of:

a) removing offsets from each of said fringe pattern images to obtain pure AMFM patterns;

b) determining contingent analytic images corresponding to each of said AMFM patterns;

c) determining phase differences from dependent pairs of said contingent analytic images; and

d) estimating phase shifts between pairs of said contingent analytic images, wherein said phase shifts between pairs of said contingent analytic images are said relative phase shifts between fringe pattern images.

2. A method as claimed in claim 1 wherein said removing step is performed by calculating interframe difference images between pairs of said fringe pattern images.

3. A method as claimed in claim 1 or 2 wherein said contingent analytic images comprise complex images with said AMFM patterns as imaginary parts and imaginary parts of a vortex operator applied to said AMFM patterns in said real parts.

4. A method as claimed in any one of claims 1 to 3 further comprising the steps of:

e) estimating a spatial phase of said fringe pattern images;

f) estimating an amplitude modulation and said offset of said fringe pattern images;

g) determining an accuracy measure of said contingent analytic images from said estimated amplitude modulation, offset and spatial phase;

h) determining a weighting function wherein areas of low accuracy measure are given a low weighting; and

i) iteratively repeating steps d) to h) by applying said weighting function in step d), until said accuracy measure is above a predetermined quantity.

5. A method as claimed in claim 4 wherein said accuracy measure determination step is performed by comparing one of said analytic images with a reconstructed fringe pattern, wherein said reconstructed fringe pattern is reconstructed using said estimated amplitude modulation, offset and spatial phase.

6. A method of estimating a spatial phase of fringe pattern images in a sequence of fringe patterns, said method comprising the steps of:

a) removing offsets from each of said fringe pattern images to obtain pure AMFM patterns;

b) determining contingent analytic images corresponding to each of said AMFM patterns;

c) determining phase differences from dependent pairs of said contingent analytic images;

d) estimating phase shifts between pairs of said contingent analytic images; and

e) estimating a spatial phase of said fringe pattern images.

7. A method as claimed in claim 6 wherein said removing step is performed by calculating interframe difference images between pairs of said fringe pattern images.

8. A method as claimed in claim 6 or 7 wherein said contingent analytic images comprise complex images with said AMFM patterns as imaginary parts and imaginary parts of a vortex operator applied to said AMFM patterns in said real parts.

9. A method as claimed in any one of claims 6 to 8 further comprising the steps of:

f) estimating an amplitude modulation and said offset of said fringe pattern images;

g) determining an accuracy measure of said contingent analytic images from said estimated amplitude modulation, offset and spatial phase;

h) determining a weighting function wherein areas of low accuracy measure are given a low weighting; and

i) iteratively repeating steps d) to h) by applying said weighting function in step d), until said accuracy measure is above a predetermined quantity.

10. A method as claimed in claim 9 wherein said accuracy measure determination step is performed by comparing one of said analytic images with a reconstructed fringe pattern, wherein said reconstructed fringe pattern is reconstructed using said estimated amplitude modulation, offset and spatial phase.

11. A method as claimed in any one of claims 1 to 10 wherein an intensity of said fringe pattern images are in the form:

$$f_n(x,y) = a(x,y) + b(x,y)\cos\left[\psi(x,y) + \delta_n\right]$$

wherein $a(x,y)$ is said offset, $b(x,y)$ is said amplitude modulation $\psi(x,y)$ is said spatial phase and δ_n is a phase shift parameter.

12. Apparatus for estimating relative phase shifts between fringe pattern images in a sequence of phase-related fringe patterns, said apparatus comprising:

means for removing offsets from each of said fringe pattern images to obtain pure AMFM patterns;

means for determining contingent analytic images corresponding to each of said AMFM patterns;

means for determining phase differences from dependent pairs of said contingent analytic images; and

means for estimating phase shifts between pairs of said contingent analytic images, wherein said phase shifts between pairs of said contingent analytic images are said relative phase shifts between fringe pattern images.

13. Apparatus as claimed in claim 12 wherein said means for removing offsets comprises means for calculating interframe difference images between pairs of said fringe pattern images.

14. Apparatus as claimed in claim 12 or 13 wherein said contingent analytic images comprise complex images with said AMFM patterns as imaginary parts and imaginary parts of a vortex operator applied to said AMFM patterns in said real parts.

15. Apparatus as claimed in any one of claims 12 to 14 further comprising:

means for estimating a spatial phase of said fringe pattern images;

means for estimating an amplitude modulation and an offset of said fringe pattern images;

means for determining an accuracy measure of said contingent analytic images from said estimated amplitude modulation, offset and spatial phase;

means for determining a weighting function wherein areas of low accuracy measure are given a low weighting; and

iterative means for providing said weighting function to said means for estimating phase shifts, until said accuracy measure is above a predetermined quantity.

16. Apparatus as claimed in claim 15 wherein said means for determining an accuracy measure comprises a comparator for comparing one of said analytic images with a reconstructed fringe pattern, wherein said reconstructed fringe pattern is reconstructed using said estimated amplitude modulation, offset and spatial phase.

17. Apparatus for estimating a spatial phase of fringe pattern images in a sequence of fringe patterns, said apparatus comprising:

means for removing offsets from each of said fringe pattern images to obtain pure AMFM patterns;

means for determining contingent analytic images corresponding to each of said AMFM patterns;

means for determining phase differences from dependent pairs of said contingent analytic images;

means for estimating phase shifts between pairs of said contingent analytic images; and

means for estimating a spatial phase of said fringe pattern images.

18. Apparatus as claimed in claim 17 wherein said means for removing offsets comprises means for calculating interframe difference images between pairs of said fringe pattern images.

19. Apparatus as claimed in claim 17 or 18 wherein said contingent analytic images comprise complex images with said AMFM patterns as imaginary parts and imaginary parts of a vortex operator applied to said AMFM patterns in said real parts.

20. Apparatus as claimed in any one of claims 17 to 19 further comprising:

means for estimating an amplitude modulation and an offset of said fringe pattern images;

means for determining an accuracy measure of said contingent analytic images from said estimated amplitude modulation, offset and spatial phase;

means for determining a weighting function wherein areas of low accuracy measure are given a low weighting; and

iterative means for providing said weighting function to said means for estimating phase shifts, until said accuracy measure is above a predetermined quantity.

21. Apparatus as claimed in claim 20 wherein said means for determining an accuracy measure comprises a comparator for comparing one of said analytic images with a reconstructed fringe pattern, wherein said reconstructed fringe pattern is reconstructed using said estimated amplitude modulation, offset and spatial phase.

22. Apparatus as claimed in any one of claims 12 to 21 wherein said fringe pattern images are in the form:

$$f_n(x,y) = a(x,y) + b(x,y)\cos\left[\psi(x,y) + \delta_n\right]$$

wherein $a(x,y)$ is said offset, $b(x,y)$ is said amplitude modulation $\psi(x,y)$ is said spatial phase and δ_n is a phase shift parameter.

23. A method of estimating relative phase shifts between fringe pattern images in a sequence of phase-related fringe patterns, said method being substantially as described herein with reference to the accompanying drawings.

24. Apparatus for estimating relative phase shifts between fringe pattern images in a sequence of phase-related fringe patterns, said apparatus being substantially as described herein with reference to the accompanying drawings.

Dated 2 August, 2000

Canon Kabushiki Kaisha

Patent Attorneys for the Applicant/Nominated Person

SPRUSON & FERGUSON

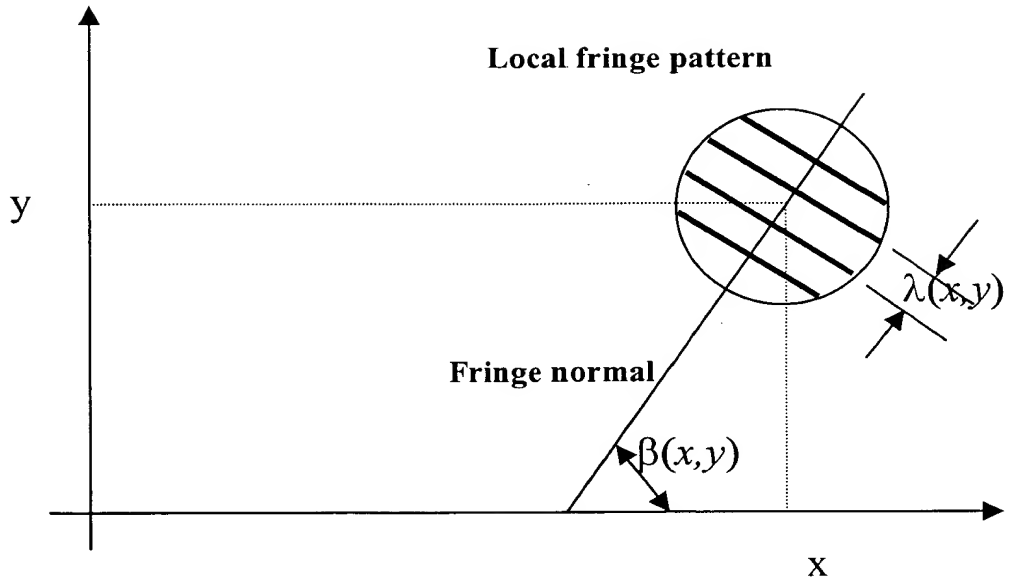

Fig. 1

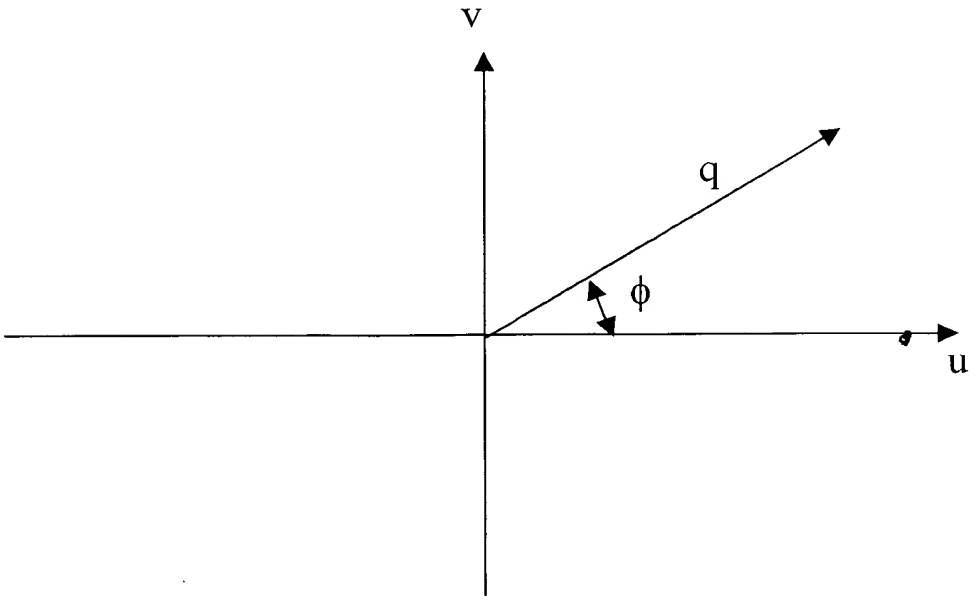

Fig. 2

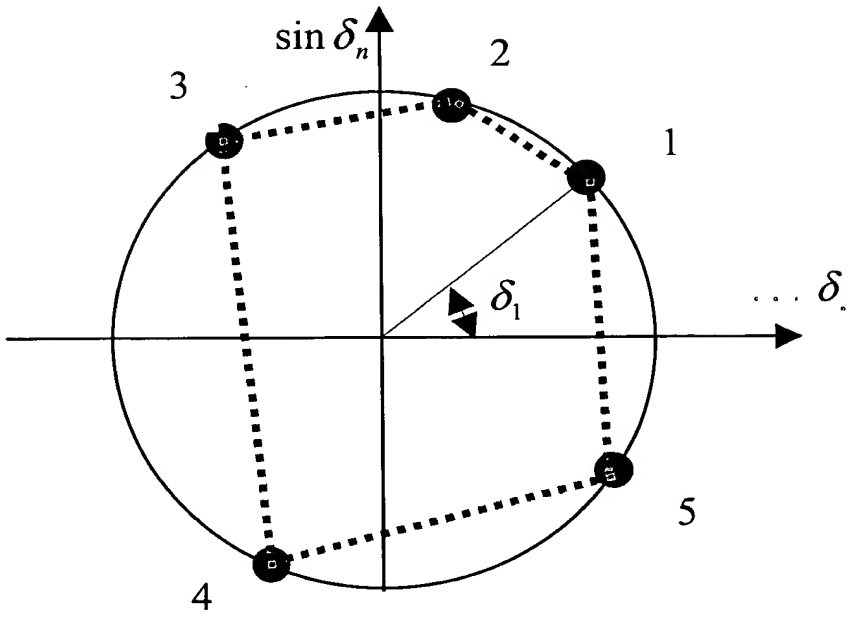

Fig. 3A

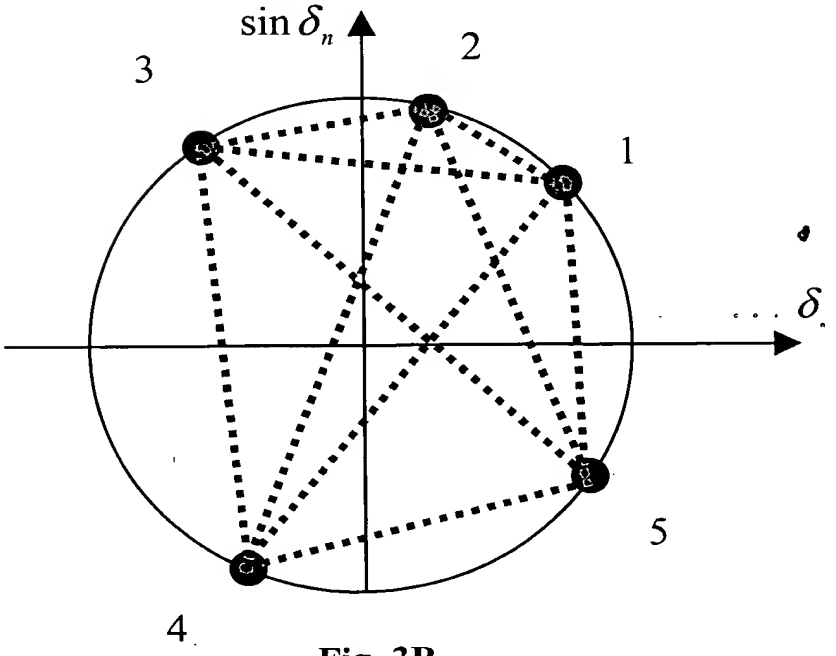

Fig. 3B

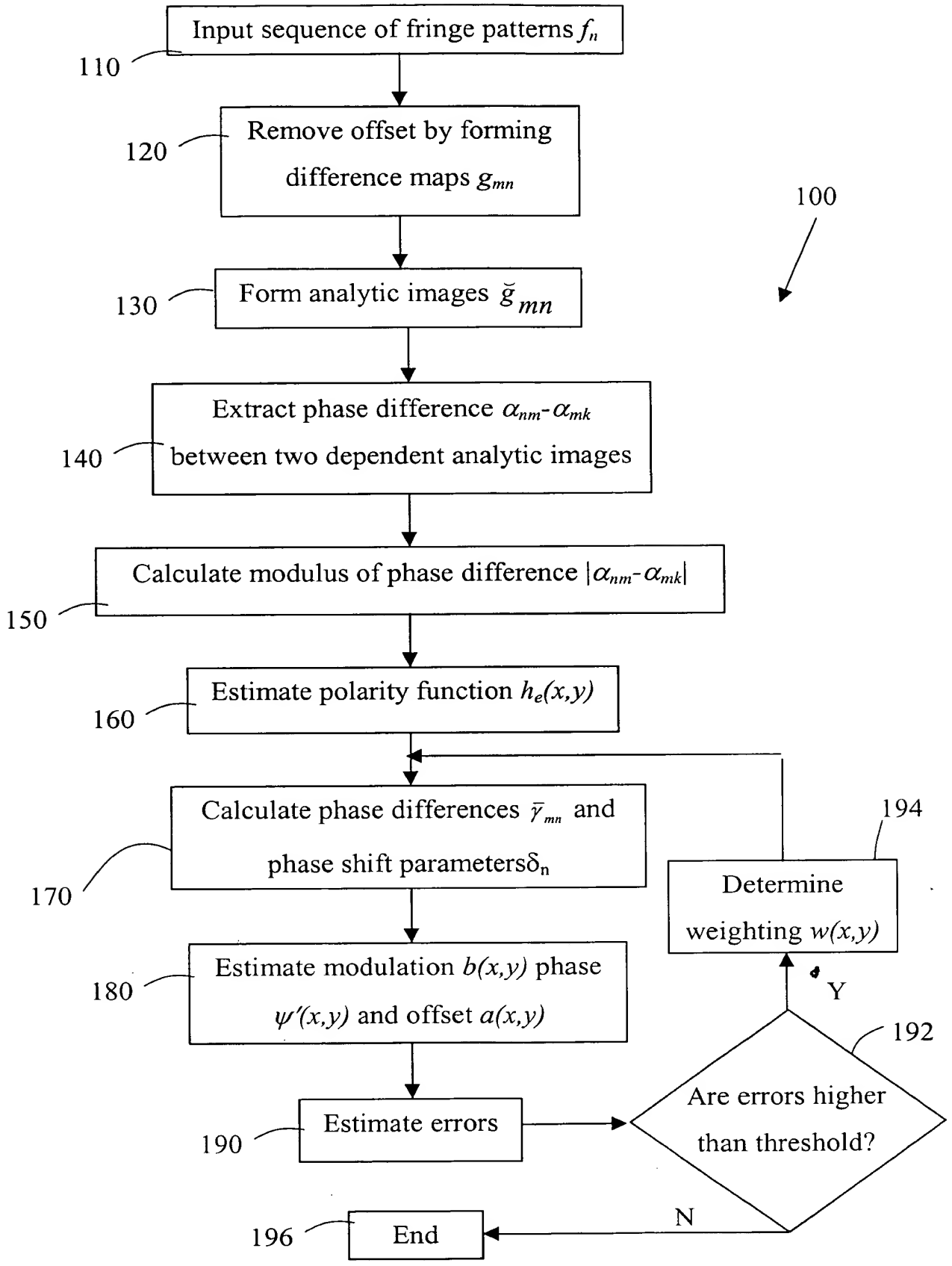
Input sequence of fringe patterns f_n
110
Remove offset by forming difference maps g_{mn}
120
100
Form analytic images $\breve{g}_{mn}$
130
Extract phase difference α_{nm}-α_{mk} between two dependent analytic images
140
Calculate modulus of phase difference $|\alpha_{nm}-\alpha_{mk}|$
150
Estimate polarity function $h_e(x,y)$
160
Calculate phase differences $\bar{\gamma}_{mn}$ and phase shift parametersδ_n
170
194
Determine weighting $w(x,y)$
Y
Estimate modulation $b(x,y)$ phase $\psi'(x,y)$ and offset $a(x,y)$
180
192
Are errors higher than threshold?
Estimate errors
190
N
196
End

Fig. 4

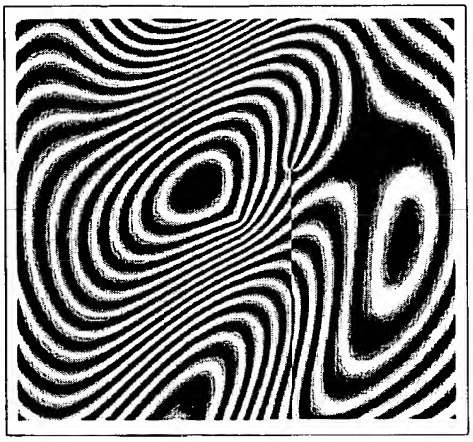

Fig. 5

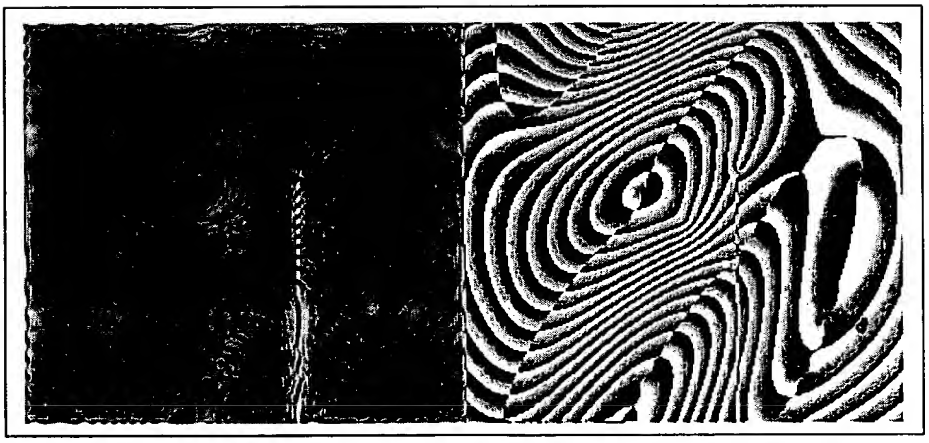

Fig. 6A

Fig. 6B

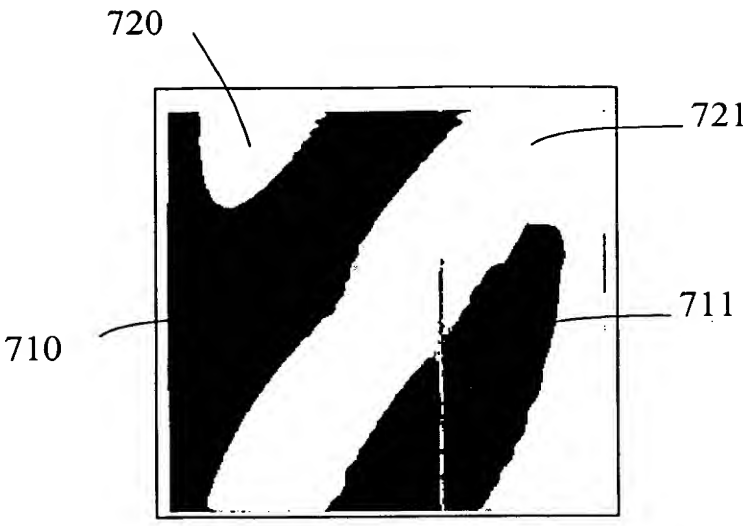
720
721
711
710

Fig. 7A

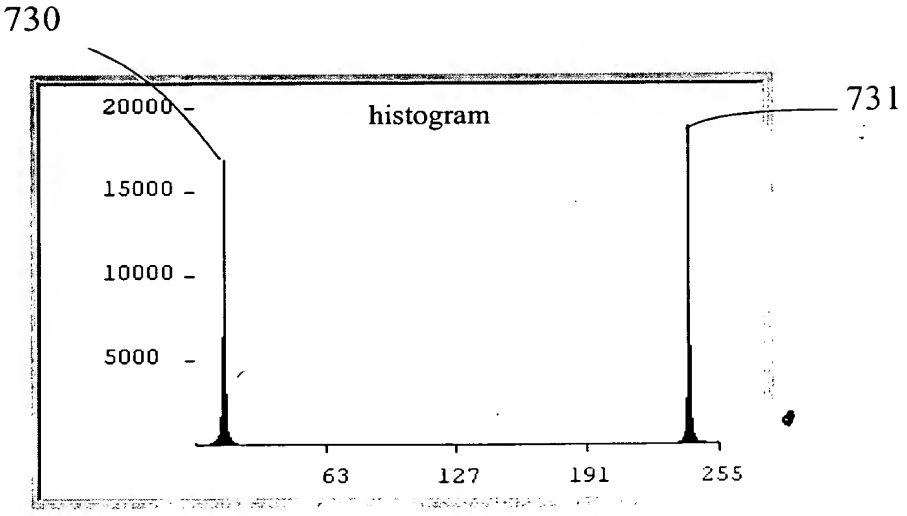
730
731
histogram
20000
15000
10000
5000
63
127
191
255

Fig. 7B

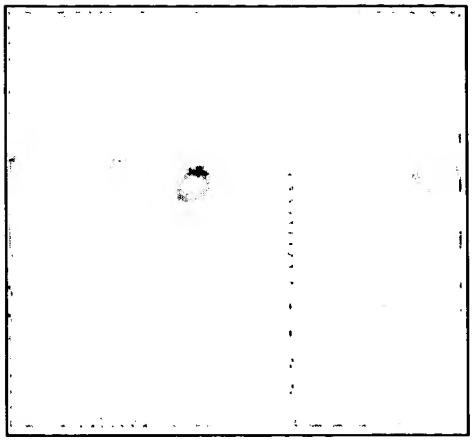

Fig. 8A

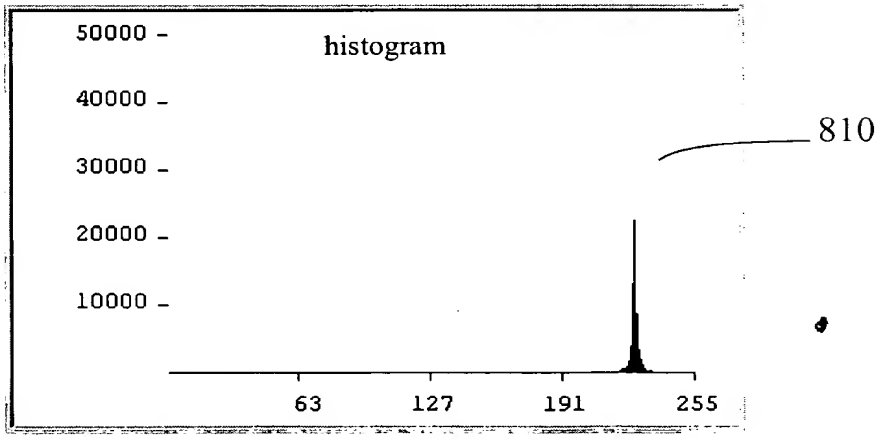

Fig. 8B

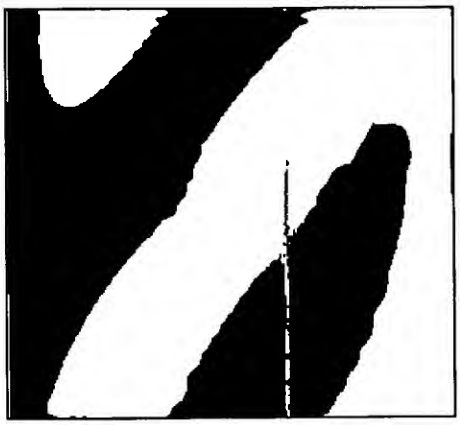

Fig. 9

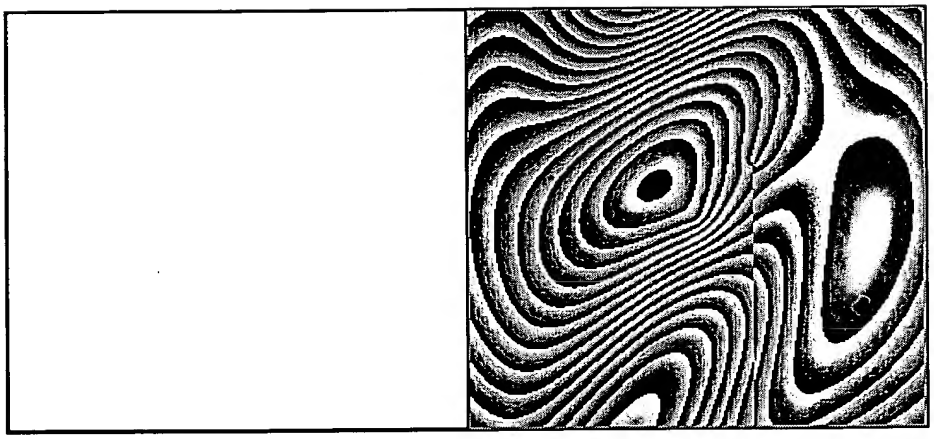

b(x,y)

Fig. 10A

ψ(x,y)

Fig. 10B

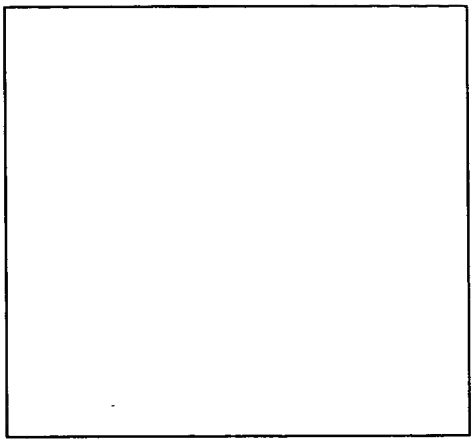

Fig. 11

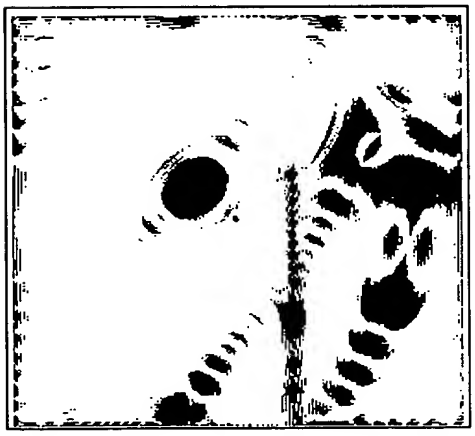

Fig. 12

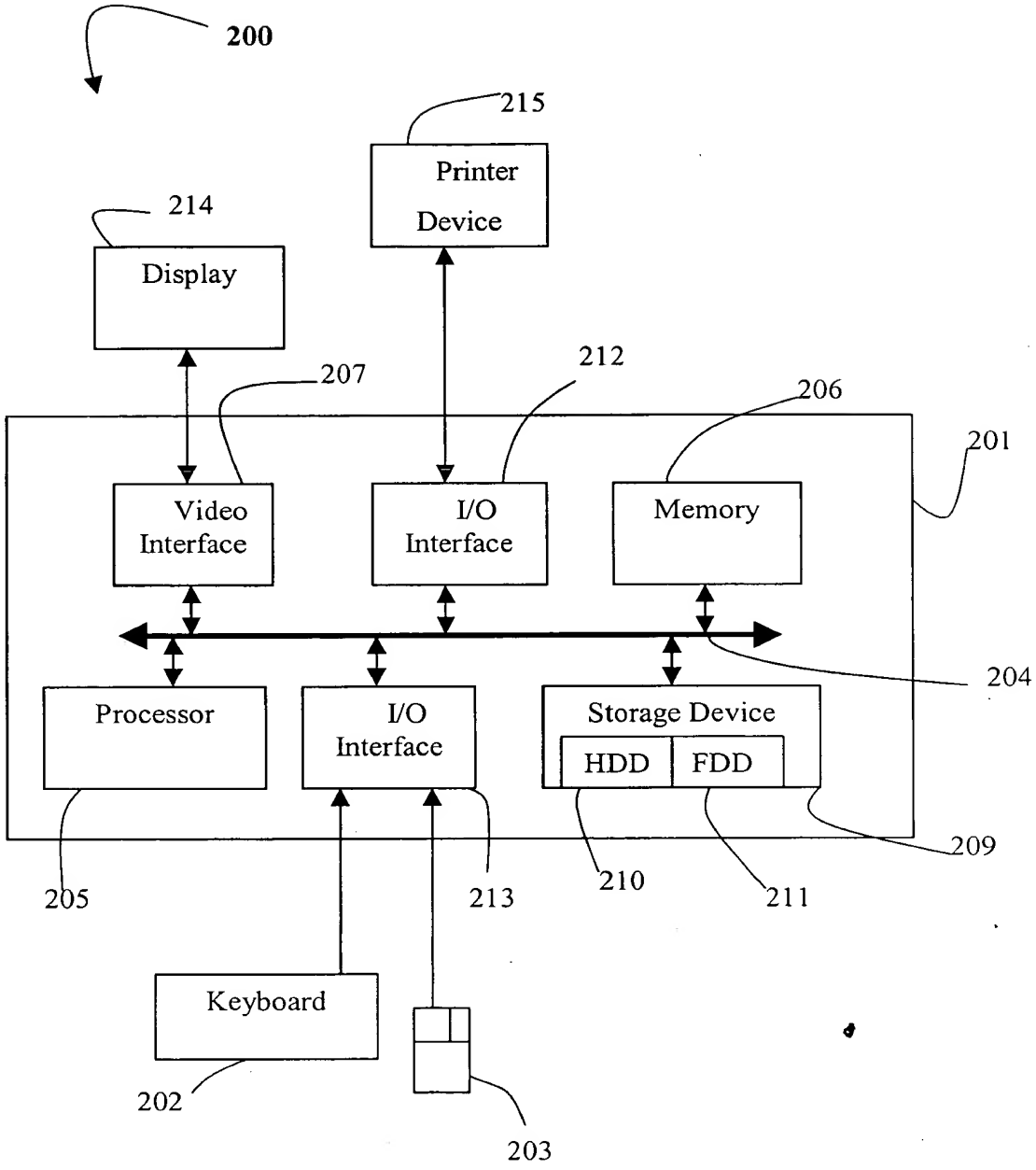
200
215
Printer Device
214
Display
207
212
206
201
Video Interface
I/O Interface
Memory
204
Processor
I/O Interface
Storage Device
HDD
FDD
209
205
213
210
211
Keyboard
202
203

Fig. 13

This Page Blank (uspto)